



Contents lists available at ScienceDirect

Journal of Electron Spectroscopy and Related Phenomena

journal homepage: www.elsevier.com/locate/elspec

Renormalized band structure of Sr₂RuO₄: A quasiparticle tight-binding approach



V.B. Zabolotnyy^{a,*}, D.V. Evtushinsky^a, A.A. Kordyuk^{a,b}, T.K. Kim^{a,c}, E. Carleschi^d, B.P. Doyle^d, R. Fittipaldi^e, M. Cuoco^e, A. Vecchione^e, S.V. Borisenko^a

^a Institute for Solid State Research, IFW-Dresden, P.O. Box 270116, D-01171 Dresden, Germany

^b Institute of Metal Physics of National Academy of Sciences of Ukraine, 03142 Kyiv, Ukraine

^c Diamond Light Source Ltd., Didcot, Oxfordshire OX11 0DE, United Kingdom

^d Department of Physics, University of Johannesburg, P.O. Box 524, Auckland Park 2006, South Africa

^e CNR-SPIN, and Dipartimento di Fisica "E.R. Caianiello", Università di Salerno, I-84084 Fisciano (Salerno), Italy

ARTICLE INFO

Article history:

Received 6 June 2013

Received in revised form 1 October 2013

Accepted 4 October 2013

Available online 21 October 2013

Keywords:

ARPES

Strontium ruthenate

Electronic band structure

Tight-binding model

Surface photoemission

ABSTRACT

We derive an effective quasiparticle tight-binding model which is able to describe with high accuracy the low-energy electronic structure of Sr₂RuO₄ obtained by means of low temperature angle resolved photoemission spectroscopy. Such an approach is applied to determine the momentum and orbital dependent effective masses and velocities of the electron quasiparticles close to the Fermi level. We demonstrate that the model can provide, among the various computable physical quantities, a very good agreement with the experimentally measured specific heat coefficient and compares well with the plasma frequency estimated from local density calculations. Its use is underlined as a realistic input in the analysis of the possible electronic mechanisms related to the superconducting state of Sr₂RuO₄.

© 2013 Elsevier B.V. All rights reserved.

1. Introduction

Since its discovery, the unconventional p-type superconductor Sr₂RuO₄ remains in the focus of solid state research [1–4]. Obtaining a precise low energy electronic structure of this material is essential for understanding many of its intricate physical properties, including superconductivity. There are generally two ways to acquire this information: either some sort of theoretical *ab initio* calculation, or a direct experimental measurement. An advantage of theoretical methods is that generally a band dispersion or a matrix element at any momentum point in the Brillouin zone can be computed as a result of a numerical scheme. However, there are known difficulties. For instance, it is hard to capture the total band renormalization with the density functional theory (DFT), and sometimes even relative band positions have to be checked against experimental data [5]. Likewise, experimental methods have inherent limitations on their part as well. Many of them measure certain integral property. In the case of transport measurements, this could be the density of states at the Fermi level, in case of de Haas–van Alphen measurements these would be the resonance frequencies

corresponding to some of the FS cross sections that can be observed in a sample of a given purity. For the Compton scattering studies, which recently gain popularity with layered superconductors, one's task is to reconstruct a 2D electron density from a set of experimentally measured Compton profiles [6–11]. Therefore, in terms of experimental band mapping [12], angle-resolved photoelectron spectroscopy appears to be the most direct energy- and momentum-resolving tool.

Though the first ARPES measurements on Sr₂RuO₄ were plagued by surface states [13–16], finally, with the exception of some finer details [17], a general agreement between photoemission and bulk probes have been achieved [18,6]. Both use of surface aging [14,19] and circularly polarized light [17] were suggested as a possible remedy for the surface problem in this material. Nonetheless, only scattered reports on integral quantities (like average Fermi velocities or effective masses) characterizing the band structure of Sr₂RuO₄ as measured in ARPES experiment are available in the literature and a detailed quantitative description of the photoemission band structure of Sr₂RuO₄ is hard to find. In this light, fitting the dispersion of the renormalized low energy quasiparticles with a tight-binding (TB) model, as it has been implemented for the layered dichalcogenides 2H-TaSe₂ and 2H-NbSe₂, appears to be a demanded step [20,21].

One of the advantages of tight-binding Hamiltonians is that they allow the band structure to be computed on very fine meshes in the

* Corresponding author. Tel.: +49 351 46 59 763.

E-mail addresses: v.zabolotnyy@gmail.com, v.zabolotnyy@ifw-dresden.de (V.B. Zabolotnyy).

Brillouin zone at low computational cost, which greatly facilitates calculation of transport, superconducting and other properties related to the fermiology [22]. Genuinely TB model is meant to describe unrenormalized noninteracting electrons. For example, TB models with corresponding sets of parameters fitting *theoretically calculated unrenormalized bands* of Sr_2RuO_4 have been reported earlier [23–26,22,27,28], and used to calculate magnetic response [29,25], Hall coefficient [27], photoemission spectra [24], or upon introduction of renormalization in accordance with de Haas–van Alphen measurements compared to photoemission [30]. However, TB models can also be successfully applied to parameterize dynamics of quasiparticles, as it has been done in the case of graphene [31], reconstructed diamond surface $\text{C}(1\ 1\ 1)2 \times 1$ [32] or in iron arsenides [33]. To avoid possible confusion, we will refer to the latter approach, describing renormalized quasiparticles, as an *quasiparticle tight-binding* and for the corresponding renormalized TB-parameters [34] a notation with tildes will be used.

2. Methods

Here we combine our experimental data with a quasiparticle tight-binding approach to produce an accurate description of the quasiparticle dispersion in single layer ruthenate Sr_2RuO_4 in the vicinity of the FL.

High-quality Sr_2RuO_4 single crystals used in this work have been grown by the flux-feeding floating-zone technique with Ru self-flux [35,36]. The composition and structure of the samples have been characterized by X-ray and electron backscatter diffraction. All the diffraction peaks had the expected (0 0 1) Bragg reflections of the Sr_2RuO_4 phase, confirming the absence of any spurious phase. The purity of the crystals is supported by a.c. susceptibility and resistivity measurements demonstrating a narrow superconducting transition with $T_c = 1.34$ K, which is a signature of a low impurity concentration [37]. Photoemission data were collected at the BESSY 1³ ARPES station equipped with a SCIENTA R4000 analyzer and a Janis ³H cryostat [38,39]. Further details on the experimental geometry and Fermi surface mapping can be found elsewhere [40,41] and in Appendix A.

3. Surface issues

Before presenting the modeling of the Sr_2RuO_4 electronic structure it is worth pointing out a few aspects which have to be considered with care in the attempt of deriving a TB description of the experimental data [20,21,42,43]. Indeed, the electronic structure of Sr_2RuO_4 as seen in photoemission experiments can be regarded as a superposition of two sets of features, one corresponding to the bulk bands, and the other one to the surface bands [44,17,24,16]. While the momentum disparity between the corresponding surface and bulk features is comparatively small at the FL, the difference becomes notable at higher binding energies because of the unequal renormalization of the surface and bulk bands [44,40,17]. To illustrate this issue in Fig. 1 we show a cut through the α pocket, where the surface and bulk α bands are well resolved, so that their MDC dispersions can be fit and traced down to about 50 meV in binding energy. We find that the velocity of the bulk band projected on the cut direction is about 1 eV Å, and does not vary much within the first 50 meV below the FL. However, for the surface band, contrary to the expectations expressed in Ref. [44], we find an abrupt change in the band velocity located at about 17 meV binding energy.

Such a kink in the band dispersion typically signals the occurrence of a coupling between electrons and bosonic modes, which at these energies are typically ascribed to phonons [45–48]. Considering the evidence for a strong electron phonon coupling in Sr_2RuO_4 ,

which is based on the neutron data by Braden et al. [49,50] and theoretical calculations [51,52], it is interesting to have a closer look at this issue. One may notice that up to 4 THz (~ 16.5 meV) there are only acoustic phonon branches, and in the range 4–5 THz weakly dispersing optical phonons of various symmetries are present, which seem to be a good candidate to cause the observed kink in the band dispersion. Such a variation in the electron–phonon coupling for the bulk and surface bands may seem surprising at first. However, the lower symmetry of the local ionic environment is likely to account for the enhanced electron–phonon coupling at the metal surface [53,54]. This dichotomy also helps to clarify the difference between the Ingle et al. [44] and Iwasawa et al. [55] reports, who showed a practically flat dispersion for the α band, on one side, and the kink reported by Aiura et al. [56] and Kim et al. [57] on the other side. In view of the current data we believe the latter two experiments must have been performed under conditions of a dominating surface component.

There are two outcomes from this observation. The first one, mainly pertaining to the current study, is that when constructing any TB fit intended to describe the bulk band structure of Sr_2RuO_4 , one always has to pick the band with a higher Fermi velocity from the two close bulk and surface features. A higher Fermi velocity for the bulk counterparts as compared to surface ones has also been observed in other layered superconductor $\text{YBaCu}_2\text{O}_{7-\delta}$ [58], which brings about the second outcome, apparently affecting band renormalization studies performed with ARPES in general. The point is that the momentum splitting between the surface and bulk bands might be negligibly small, hence treating an unresolved composite feature as a single one may lead to an underestimated Fermi velocity (overestimated renormalization) as contrasted to the true bulk values.

4. Results and discussion

Let us consider the effective TB model. In comparison to many other layered superconductors Sr_2RuO_4 is known to have a relatively weak k_z dispersion [59–63], which is still further reduced by the spin–orbit interaction [64]. Therefore, in choosing an appropriate variety of TB model for Sr_2RuO_4 we neglect the k_z dispersion and follow the basic formulation already proposed by Ng et al. as well as by other authors [65,66,2,67]. In this framework, the TB Hamiltonian can be expressed as follows:

$$H = \sum_{\vec{k}, s} \psi_s^\dagger(\vec{k}) \hat{A}(\vec{k}, s) \psi_s(\vec{k}) + \text{h.c.}, \quad (1)$$

where $\psi_s(\vec{k}) = [d_s^{yz}(\vec{k}), d_s^{xz}(\vec{k}), d_{-s}^{xy}(\vec{k})]^T$ indicates the basis with a three-component spinor and the matrix $\hat{A}(\vec{k}, s)$ is given by

$$\hat{A}(\vec{k}, s) = \begin{pmatrix} \epsilon_k^{yz} - \tilde{\mu} & \epsilon_k^{\text{off}} + is\lambda & -s\lambda \\ \epsilon_k^{\text{off}} - is\lambda & \epsilon_k^{xz} - \tilde{\mu} & i\lambda \\ -s\lambda & -i\lambda & \epsilon_k^{xy} - \tilde{\mu} \end{pmatrix}, \quad (2)$$

and

$$\begin{aligned} \epsilon_k^{yz} &= -2\tilde{t}_2 \cos(k_x) - 2\tilde{t}_1 \cos(k_y); \quad \epsilon_k^{xz} = -2\tilde{t}_1 \cos(k_x) \\ &\quad - 2\tilde{t}_2 \cos(k_y); \quad \epsilon_k^{xy} = -2\tilde{t}_3 (\cos(k_x) + \cos(k_y)) \\ &\quad - 4\tilde{t}_4 \cos(k_x) \cos(k_y) - 2\tilde{t}_5 (\cos(2k_x) \\ &\quad + \cos(2k_y)); \quad \epsilon_k^{\text{off}} = -4\tilde{t}_6 \sin(k_x) \sin(k_y). \end{aligned}$$

In Fig. 2 we fit the model parameters in order to optimally reproduce the experimental data in an energy window close to

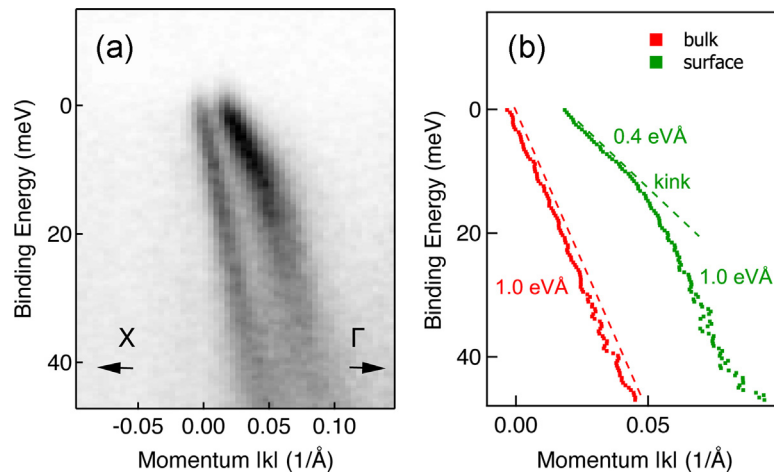


Fig. 1. Surface and bulk α bands (a) and their MDC dispersions (b). The projections of the band velocities were estimated by fitting a line to a straight segments of experimental dispersion. Since the cut is not perpendicular to the Fermi surface locus, the total in-plane velocities are actually larger. The data were collected with $h\nu = 35$ eV at $T = 1$ K.

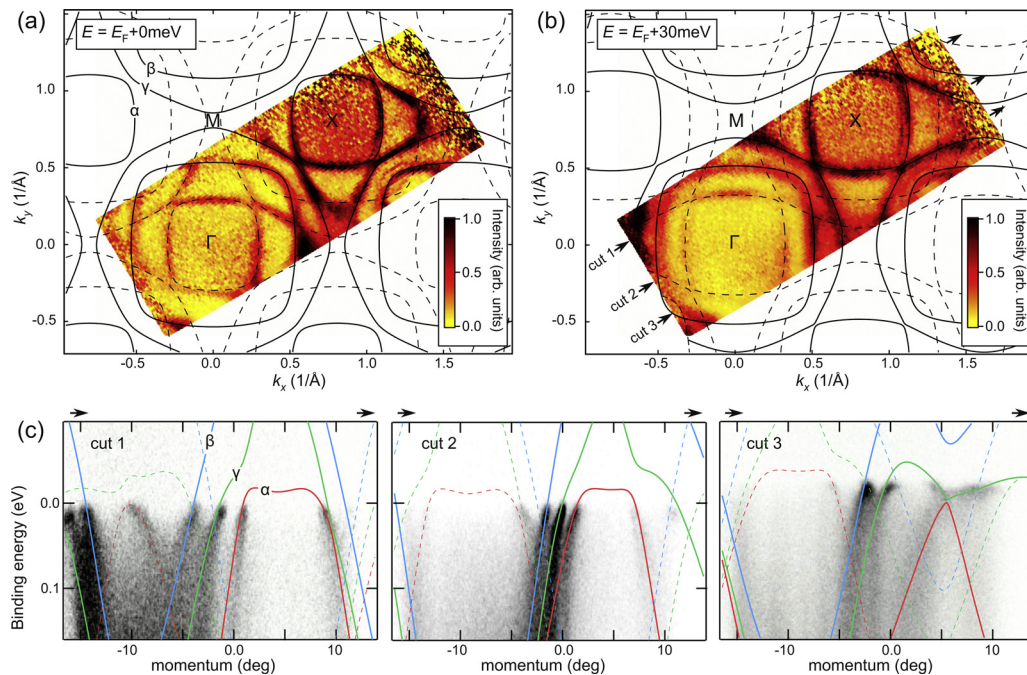


Fig. 2. Comparison between the developed TB-fit and experimentally observed low energy quasiparticles, demonstrating agreement for $E_{\text{Bind}} \lesssim 30$ meV. (a) Experimental Fermi surface of Sr_2RuO_4 with superimposed TB contours. (b) Intensity distribution similar to the Fermi surface map shown in (a), but taken 30 meV below the FL. (c) Comparison of experimental intensity distribution for several energy–momentum cuts with fitted quasiparticle dispersion. Cuts position in momentum space is marked by small arrows in panel (b). Solid lines correspond to the main α , β and γ bands, while the dotted contours denote their respective replicas, which are shifted by $Q = (\pi, \pi)$ with respect to their original bands. The data were collected with $h\nu = 80$ eV at $T = 1.8$ K.

the FL.¹ Technical details on the fitting procedure can be found in Appendix A. Panel (a) shows the TB-model Fermi surface contours superimposed over the experimental data. The effective electronic parameters which provide the best description for the dispersion of the low energy quasiparticles in Sr_2RuO_4 can be summarized in the following table:

$\tilde{\lambda}$	\tilde{t}_1	\tilde{t}_2	\tilde{t}_3	\tilde{t}_4	\tilde{t}_5	\tilde{t}_6	$\tilde{\mu}$
0.032	0.145	0.016	0.081	0.039	0.005	0.000	0.122

¹ Since the model is degenerate in spin s , either $s = -1$ or $s = 1$ can be used to obtain dispersions.

Having at hand simple equations describing the band dispersion it is easy to calculate the density of states (DOS) and make an estimate for the electron count and electronic specific heat [68]. To calculate DOS we used tetrahedron method of Lehmann and Taut [69]. The results are shown in Fig. 3. The estimated density of states at the FL for the three low energy bands are as follows: $g_\alpha \approx 3.4$, $g_\beta \approx 3.0$ and $g_\gamma \approx 10.5$ states/eV molRu, which totals to $g \approx 16.9$ states/eV molRu and translates to the Sommerfeld coefficient of 40 mJ/K² molRu. The obtained number is in agreement with the experimentally measured values ranging from 29 to 45.6 mJ/K² molRu [70–79], which indicates that the developed fit properly describes the dispersion of the bulk bands in the vicinity of the FL. The integral of the DOS up to the FL gives the electron count of 3.9 electrons per BZ, which again, within the experimental accuracy, agrees with the expected 4 electrons per BZ.

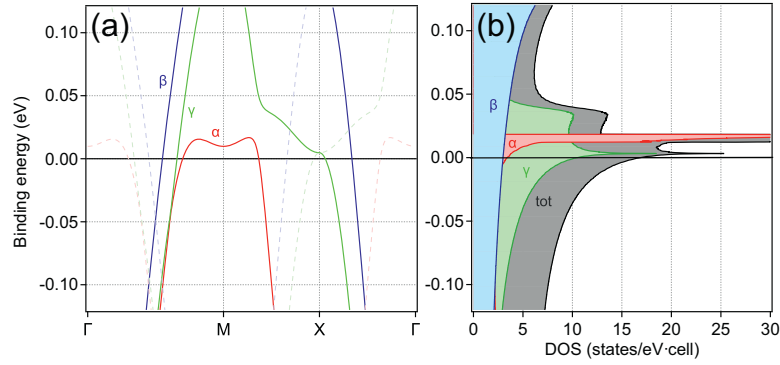


Fig. 3. Dispersion of the quasiparticle TB bands (a) and the derived quasiparticle density of states (b) in the vicinity of the FL. The dotted lines are the replicas of the original bands shifted by vector $Q=(\pi, \pi)$.

Electronic structure of materials is frequently discussed in terms of effective masses. Such a reduction to a single integral value m^* enables a comparison between various experimental and theoretical methods. In this context, it is useful to remind that besides the band mass tensor $m_{\mu,\nu} = \hbar^2(\partial^2\epsilon(\mathbf{k})/\partial k_\mu\partial k_\nu)^{-1}$ different effective masses are frequently considered: (1) the band mass m_b as it can be obtained from the bare electronic dispersion, (2) the thermodynamic mass m^* , (3) the cyclotron resonance mass m_c , (4) the susceptibility mass m_{suscept}^* , (5) the plasma frequency mass m_p [18,80]. Here, the quasiparticle densities of states can be easily recalculated into thermodynamic masses ($m^*/m_e = \pi \hbar^2 g/m_e a^2$) and compared, on the band by band basis, to the thermodynamic masses reported in de Haas–van Alphen measurements as summarized in the table below.

Mass type	α	β	γ	Total	Year
This study	5.4	4.8	16.7	26.9	
Cyclotron thermodynamic [81,18]	3.3	7.0	16.0	26.3	2001
Cyclotron thermodynamic [77]	3.4	7.5	14.6	25.5	1998
Cyclotron thermodynamic [82]	3.4	6.6	12.0	22.0	1996
Cyclotron thermodynamic [83]	3.2	6.6	12.0	21.8	1996
Cyclotron resonance [18]	2.1	4.3	5.8	12.2	2003
Cyclotron resonance [84]	4.3	5.8	9.7	19.8	2000

As one may notice there is a gradual increase of the total thermodynamic mass reported by the de Haas–van Alphen measurements with time, which is probably related to the improving

quality of available crystals. Our total mass ($26.9m_e$) is closest to the most recent dHvA value of $26.3m_e$. Similarly, we find a good correspondence for the mass of the γ band, however there seems to be a difference in the masses of the α and β bands. While in the current fit these bands have practically the same mass, in the de Haas–van Alphen data their mass ratio is about two. In the two-dimensional case the density of states, and hence the effective mass, is inversely proportional to the Fermi velocity and directly proportional to the length of the Fermi surface contour. Therefore, assuming equal velocities for the α and β band would give a mass of the β band to be twice that of the α band, as the average radius of the β band is about twice as high. As clarified in Ref. [18, p. 686] this assumption was ‘actually used... as a guiding line’ when extracting the susceptibility effective mass. Nevertheless, as can be seen from Fig. 3a, the quasiparticle Fermi velocity of the α band is systematically lower than that for the β band, and the accurate account of the variation of the Fermi velocity, v_F , and k_F yields about the same thermodynamic masses for the α and β bands. We expect that the value extracted from the presented TB model correctly reproduces the relation between the effective mass of the α and β bands.

Besides the heat capacity, the obtained effective TB model can be used to calculate other averaged properties over the Brillouin zone, such as the plasma frequency, whose value is given by

$$\hbar\Omega_{xx} = \sqrt{\sum_{i=\alpha,\beta,\gamma} \frac{e^2}{L_a L_b L_c \epsilon_0} \langle \int k \frac{\partial^2 E^{(i)}}{\partial k_x \partial k_x} \rangle_{\text{BZ}}}. \quad (3)$$

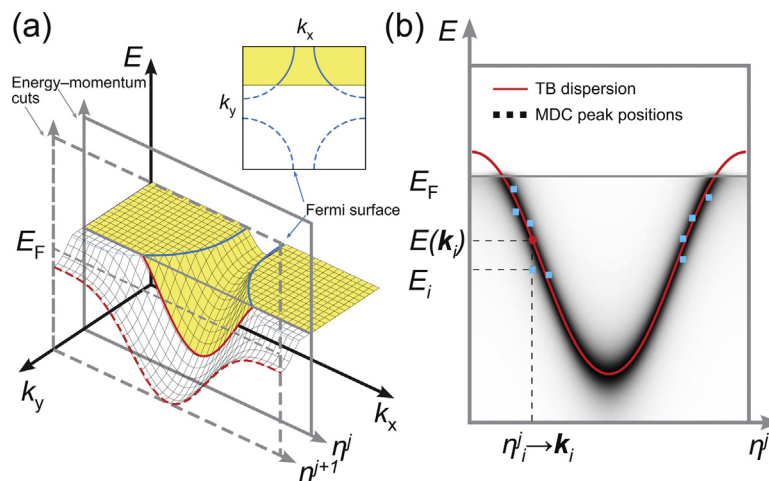


Fig. 4. A cartoon explaining Fermi surface mapping (a) and technical details of the TB fit procedure (b). For details, see Appendix A.

from where we get $\hbar\Omega_{xx} = 1.3$ eV. The value is about 3.5 times smaller than the one based on the unrenormalized band structure calculation [85]. This comparison, however, has to be taken with a grain of salt. First we are comparing to the results of LDA calculation, not to direct experimental data. Second, unlike the Sommerfeld coefficient, plasma frequency depends not only on the dispersion of the quasiparticles at the Fermi level but on the whole dispersion. In this regard a whole energy parametrization is desired, but currently it is hard to realize. It is well known that the velocity of the electronic bands in cuprates, ruthenates and other materials barely remains constant. In certain cases there are even abrupt changes known as kinks. Therefore to produce a description of the electronic structure both at low and high binding energies one has to abandon the quasiparticle description and think in terms of spectral function $A(\mathbf{k}, \omega)$ and the related to it self-energy. For the systems with relatively simple electronic structure this can be done in practice, Bi-2212 can be considered as a good example [86]. However Sr₂RuO₄ has much richer band structure, which is additionally complicated by the coexistence of bulk and surface bands, therefore we had to limit ourself to a technically feasible task, which is the description of the quasiparticle in the vicinity of the Fermi level.

5. Conclusions

We have developed an effective tight-binding model that captures the low energy electronic features of the quasiparticle spectra of Sr₂RuO₄ taking ARPES data as an input. Owing to different degree of renormalization in the bulk and at the surface, the bulk bands have been properly selected and analyzed for the determination of the quasiparticle model. We have extracted the momentum and orbital dependence of the Fermi velocity and of the effective masses close to the FL. As a demonstration of the use of the derived model, we have calculated the density of states and found a good agreement between the Sommerfeld coefficient calculated based on the obtained fit and the one directly measured.

In a certain sense, the model is comparable to the famous fit to the de Haas–van Alphen data by Bergeman et al. [18], but owing to specifics of ARPES it benefits from three advantages: (1) unlike the dHvA, the form of the Fermi surface does not have to be reconstructed from a set of cross-sectional areas, but rather each momentum point (k_x , k_y) is probed directly; similarly, the dispersion (hence the Fermi velocity) of the low energy quasiparticles for each k -point is captured directly in ARPES energy–momentum cuts, thus it does not have to be inferred from fits to Landau–Kosevich formula [82,83], which gives only an averaged over the Fermi surface estimate for the effective mass or the Fermi velocity; (3) instead of doing a parametric fit in polar coordinates that would capture only the form of the FS, we rely on a TB-Hamiltonian, which allows easy estimates for the orbital character of the quasiparticles and their momentum dependent velocities.

We believe that the developed model can be of value for a more realistic input to compute the orbital dependent magnetic properties in order to test, for example, the relevance of the ferromagnetic or antiferromagnetic fluctuations in settling the spin-triplet pairing in the superconducting phase of Sr₂RuO₄ [87,88,2,89].

Acknowledgments

The work was supported by DFG grant ZA654/1-1. E.C. and B.P.D. thank the Faculty of Science at the University of Johannesburg for travel funding. M.C., R.F. and A.V. acknowledge support and funding from the FP7/2007-2013 under grant agreement N.264098-MAMA.

Appendix A.

This section is intended for those who are interested in technical details of the TB fit employed in this work. To understand the method, one first has to be acquainted with the basics of modern photoemission experiments and mapping of the energy–momentum space. The basic “data-unit” in ARPES experiments is a so-called energy–momentum cut, which can be considered as a slice or a cut through the 3D space spanned over the photoelectron energy E and two components of photoelectron momentum k_x and k_y . In Fig. 4a such two slices are shown by solid and dotted gray frames. Gradually changing sample orientation allows one to move the cut through the reciprocal space and obtain a fine slicing $\{\eta^0, \dots, \eta^j, \eta^{j+1}, \dots, \eta^N\}$ of the energy–momentum space covering complete 1st Brillouin zone or more. Generally the axis η^j does not have to be parallel to either k_x or k_y , as it is the case for the actual data shown in Fig. 2. Nonetheless the local coordinates of any feature in each slice η^j $\{E_i, \eta_i^j\}$ can be easily recalculated into the absolute position within the 1st Brillouin zone $\{E_i, \mathbf{k}_i\}$ and compared to the corresponding eigenvalue $E(\mathbf{k}_i)$ of the TB model. To build the model we analyze all the energy–momentum cuts that comprise the map shown in Fig. 2 by considering well defined features and determining their positions from the momentum distribution curves, where possible. Schematically these points are shown in Fig. 4b by blue squares with exaggerated noise scattering. First a visual comparison between the experimental data and the fitting dispersions was used for the manual generation of the “initial guess” for the TB parameters, which later was improved by minimizing a numerical fitness norm using standard automatic fitting routines. As fitness norm we use an averaged deviation between the experimentally determined points $\{E_i, \mathbf{k}_i\}$ and the prediction of the TB model $E(\mathbf{k})$:

$$\xi = \frac{1}{N} \sum_{i=0}^{N-1} |E_i - E(\mathbf{k}_i)|. \quad (4)$$

According to this norm the averaged deviation between the experimental MDC points and the fitting dispersion is about 6 meV, which is comparable to the energy resolution of the input data.

References

- [1] J.P. Carlo, T. Goko, I.M. Gat-Malureanu, P.L. Russo, A.T. Savici, A.A. Aczel, G.J. MacDougall, J.A. Rodriguez, T.J. Williams, G.M. Luke, C.R. Wiebe, Y. Yoshida, S. Nakatsui, Y. Maeno, T. Taniguchi, Y.J. Uemura, Nat. Mater. 11 (2012) 323.
- [2] C.M. Puetter, H.-Y. Kee, Europhys. Lett. 98 (2012) 27010.
- [3] Y. Maeno, S. Kittaka, T. Nomura, S. Yonezawa, K. Ishida, J. Phys. Soc. Jpn. 81 (2012) 011009.
- [4] K.I. Wysokiński, J.F. Annett, B.L. Györfi, Phys. Rev. Lett. 108 (2012) 077004.
- [5] J. Geck, S.V. Borisenko, H. Berger, H. Eschrig, J. Fink, M. Knupfer, K. Koepernik, A. Koitzsch, A.A. Kordyuk, V.B. Zabolotnyy, B. Büchner, Phys. Rev. Lett. 99 (2007) 046403.
- [6] N. Hiraoka, T. Buslaps, V. Honkimäki, T. Nomura, M. Itou, Y. Sakurai, Z.Q. Mao, Y. Maeno, Phys. Rev. B 74 (2006) 100501.
- [7] N. Hiraoka, A. Deb, M. Itou, Y. Sakurai, Z.Q. Mao, Y. Maeno, Phys. Rev. B 67 (2003) 094511.
- [8] P.E. Mijnarends, A. Bansil, Phys. Rev. B 13 (1976) 2381–2390.
- [9] W. Al-Sawai, B. Barbiellini, Y. Sakurai, M. Itou, P.E. Mijnarends, R.S. Markiewicz, S. Kaprzyk, S. Wakimoto, M. Fujita, S. Basak, H. Lin, Y.J. Wang, S.W.H. Eijt, H. Schut, K. Yamada, A. Bansil, Phys. Rev. B 85 (2012) 115109.
- [10] C. Uffeld, J. Laverock, T.D. Haynes, S.B. Dugdale, J.A. Duffy, M.W. Butchers, J.W. Taylor, S.R. Giblin, J.G. Analytis, J.-H. Chu, I.R. Fisher, M. Itou, Y. Sakurai, Phys. Rev. B 81 (2010) 064509.
- [11] Y. Sakurai, M. Itou, B. Barbiellini, P.E. Mijnarends, R.S. Markiewicz, S. Kaprzyk, J.-M. Gillet, S. Wakimoto, M. Fujita, S. Basak, Y.J. Wang, W. Al-Sawai, H. Lin, A. Bansil, K. Yamada, Science 332 (2011) 698–702.
- [12] E.E. Krasovskii, V.N. Strocov, N. Barrett, H. Berger, W. Schattke, R. Claessen, Phys. Rev. B 75 (2007) 045432.
- [13] T. Yokoya, A. Chainani, T. Takahashi, H. Katayama-Yoshida, M. Kasai, Y. Tokura, Phys. Rev. Lett. 76 (1996) 3009–3012.
- [14] A. Damascelli, K.M. Shen, D.H. Lu, Z.-X. Shen, Phys. Rev. Lett. 87 (2001) 239702.
- [15] A. Liesch, Phys. Rev. Lett. 87 (2001) 239701.

- [16] A. Damascelli, D.H. Lu, K.M. Shen, N.P. Armitage, F. Ronning, D.L. Feng, C. Kim, Z.-X. Shen, T. Kimura, Y. Tokura, Z.Q. Mao, Y. Maeno, *Phys. Rev. Lett.* **85** (2000) 5194–5197.
- [17] V.B. Zabolotnyy, E. Carleschi, T.K. Kim, A.A. Kordyuk, J. Trinckauf, J. Geck, D. Evtushinsky, B.P. Doyle, R. Fittipaldi, M. Cuoco, A. Vecchione, B. Büchner, S.V. Borisenko, *New J. Phys.* **14** (2012) 063039.
- [18] C. Bergemann, A.P. Mackenzie, S.R. Julian, D. Forsythe, E. Ohmichi, *Adv. Phys.* **52** (2003) 639–725.
- [19] Y. Pennec, N.J.C. Ingle, I.S. Elfimov, E. Varene, Y. Maeno, A. Damascelli, J.V. Barth, *Phys. Rev. Lett.* **101** (2008) 216103.
- [20] D.S. Inosov, D.V. Evtushinsky, V.B. Zabolotnyy, A.A. Kordyuk, B. Büchner, R. Follath, H. Berger, S.V. Borisenko, *Phys. Rev. B* **79** (2009) 125112.
- [21] D.S. Inosov, V.B. Zabolotnyy, D.V. Evtushinsky, A.A. Kordyuk, B. Büchner, R. Follath, H. Berger, S.V. Borisenko, *New J. Phys.* **10** (2008) 125027.
- [22] I.I. Mazin, D.A. Papaconstantopoulos, D.J. Singh, *Phys. Rev. B* **61** (2000) 5223–5228.
- [23] I.I. Mazin, D.J. Singh, *Phys. Rev. Lett.* **79** (1997) 733–736.
- [24] A. Liebsch, A. Lichtenstein, *Phys. Rev. Lett.* **84** (2000) 1591–1594.
- [25] D.K. Morr, P.F. Trautman, M.J. Graf, *Phys. Rev. Lett.* **86** (2001) 5978–5981.
- [26] T. Mishonov, E. Penev, *J. Phys.: Condens. Matter* **12** (2000) 143.
- [27] C. Noce, M. Cuoco, *Phys. Rev. B* **59** (1999) 2659–2666.
- [28] C. Noce, T. Xiang, *Physica C* **282** (1997) 1713–1714.
- [29] M. Braden, Y. Sidis, P. Bourges, P. Pfeuty, J. Kulda, Z. Mao, Y. Maeno, *Phys. Rev. B* **66** (2002) 064522.
- [30] K.M. Shen, N. Kikugawa, C. Bergemann, L. Balicas, F. Baumberger, W. Meevasana, N.J.C. Ingle, Y. Maeno, Z.-X. Shen, A.P. Mackenzie, *Phys. Rev. Lett.* **99** (2007) 187001.
- [31] A. Grüneis, C. Attacalite, L. Wirtz, H. Shiozawa, R. Saito, T. Pichler, A. Rubio, *Phys. Rev. B* **78** (2008) 205425.
- [32] M. Marsili, O. Pulci, F. Bechstedt, R. Del Sole, *Phys. Rev. B* **78** (2008) 205414.
- [33] R. Beaird, I. Vekhter, J.-X. Zhu, *Phys. Rev. B* **86** (2012) 140507.
- [34] L. Hozoi, S. Nishimoto, C. de Graaf, *Phys. Rev. B* **75** (2007) 174505.
- [35] R. Fittipaldi, D. Sisti, A. Vecchione, S. Pace, *Cryst. Growth Des.* **7** (2007) 2495–2499.
- [36] Z. Mao, Y. Maeno, H. Fukazawa, *Mater. Res. Bull.* **35** (2000) 1813–1824.
- [37] N. Kikugawa, A.P. Mackenzie, Y. Maeno, *J. Phys. Soc. Jpn.* **72** (2003) 237.
- [38] S.V. Borisenko, *Synchrotron Radiat. News* **25** (2012) 6–11.
- [39] S.V. Borisenko, V.B. Zabolotnyy, A.A. Kordyuk, D.V. Evtushinsky, T.K. Kim, E. Carleschi, B.P. Doyle, R. Fittipaldi, M. Cuoco, A. Vecchione, H. Berger, *J. Vis. Exp.* **68** (2012) e50129.
- [40] V.B. Zabolotnyy, S.V. Borisenko, A.A. Kordyuk, D.S. Inosov, A. Koitzsch, J. Geck, J. Fink, M. Knupfer, B. Büchner, S.-L. Drechsler, V. Hinkov, B. Keimer, L. Patthey, *Phys. Rev. B* **76** (2007) 024502.
- [41] D.S. Inosov, R. Schuster, A.A. Kordyuk, J. Fink, S.V. Borisenko, V.B. Zabolotnyy, D.V. Evtushinsky, M. Knupfer, B. Büchner, R. Follath, H. Berger, *Phys. Rev. B* **77** (2008) 212504.
- [42] A.A. Kordyuk, S.V. Borisenko, M. Knupfer, J. Fink, *Phys. Rev. B* **67** (2003) 064504.
- [43] D.V. Evtushinsky, D.S. Inosov, G. Urbanik, V.B. Zabolotnyy, R. Schuster, P. Sass, T. Hänke, C. Hess, B. Büchner, R. Follath, P. Reutler, A. Revcolevschi, A.A. Kordyuk, S.V. Borisenko, *Phys. Rev. Lett.* **105** (2010) 147201.
- [44] N.J.C. Ingle, K.M. Shen, F. Baumberger, W. Meevasana, D.H. Lu, Z.-X. Shen, A. Damascelli, S. Nakatsuji, Z.Q. Mao, Y. Maeno, T. Kimura, Y. Tokura, *Phys. Rev. B* **72** (2005) 205114.
- [45] S. Engelsberg, J.R. Schrieffer, *Phys. Rev.* **131** (1963) 993–1008.
- [46] A.W. Sandvik, D.J. Scalapino, N.E. Bickers, *Phys. Rev. B* **69** (2004) 094523.
- [47] A.A. Kordyuk, V.B. Zabolotnyy, D.V. Evtushinsky, T.K. Kim, I.V. Morozov, M.L. Kulić, R. Follath, G. Behr, B. Büchner, S.V. Borisenko, *Phys. Rev. B* **83** (2011) 134513.
- [48] D.J. Rahn, S. Hellmann, M. Kalläne, C. Sohrt, T.K. Kim, L. Kipp, K. Rossnagel, *Phys. Rev. B* **85** (2012) 224532.
- [49] M. Braden, W. Reichardt, S. Nishizaki, Y. Mori, Y. Maeno, *Phys. Rev. B* **57** (1998) 1236–1240.
- [50] M. Braden, W. Reichardt, Y. Sidis, Z. Mao, Y. Maeno, *Phys. Rev. B* **76** (2007) 014505.
- [51] T. Bauer, C. Falter, *J. Phys.: Condens. Matter* **21** (2009) 395701.
- [52] Y. Wang, J.J. Wang, J.E. Saal, S.L. Shang, L.-Q. Chen, Z.-K. Liu, *Phys. Rev. B* **82** (2010) 172503.
- [53] E. Plummer, J. Shi, S.-J. Tang, E. Rotenberg, S. Kevan, *Prog. Surf. Sci.* **74** (2003) 251–268.
- [54] I. Mazin, S. Rashkeev, *Solid State Commun.* **68** (1988) 93–95.
- [55] H. Iwasawa, Y. Aiura, T. Saitoh, I. Hase, S.I. Ikeda, Y. Yoshida, H. Bando, M. Higashiguchi, Y. Miura, X.Y. Cui, K. Shimada, H. Namatame, M. Taniguchi, *Phys. Rev. B* **72** (2005) 104514.
- [56] Y. Aiura, Y. Yoshida, I. Hase, S.I. Ikeda, M. Higashiguchi, X.Y. Cui, K. Shimada, H. Namatame, M. Taniguchi, H. Bando, *Phys. Rev. Lett.* **93** (2004) 117005.
- [57] C. Kim, W. Kyung, S. Park, C. Leem, D. Song, Y. Kim, S. Choi, W. Jung, Y. Koh, H. Choi, Y. Yoshida, R. Moore, Z.-X. Shen, C. Kim, *J. Phys. Chem. Solids* **72** (2011) 556–558.
- [58] V.B. Zabolotnyy, A.A. Kordyuk, D. Evtushinsky, V.N. Strocov, L. Patthey, T. Schmitt, D. Haug, C.T. Lin, V. Hinkov, B. Keimer, B. Büchner, S.V. Borisenko, *Phys. Rev. B* **85** (2012) 064507.
- [59] R.S. Markiewicz, S. Sahrakorpi, M. Lindroos, H. Lin, A. Bansil, *Phys. Rev. B* **72** (2005) 054519.
- [60] H. Eschrig, K. Koepernik, *Phys. Rev. B* **80** (2009) 104503.
- [61] T. Takeuchi, T. Kondo, T. Kitao, H. Kaga, H. Yang, H. Ding, A. Kaminski, J.C. Campuzano, *Phys. Rev. Lett.* **95** (2005) 227004.
- [62] A. Bansil, M. Lindroos, S. Sahrakorpi, R.S. Markiewicz, *Phys. Rev. B* **71** (2005) 012503.
- [63] K. Rossnagel, N.V. Smith, *Phys. Rev. B* **76** (2007) 073102.
- [64] M.W. Haverkort, I.S. Elfimov, L.H. Tjeng, G.A. Sawatzky, A. Damascelli, *Phys. Rev. Lett.* **101** (2008) 026406.
- [65] K.K. Ng, M. Sgrist, *Europhys. Lett.* **49** (2000) 473.
- [66] C.M. Puetter, J.G. Rau, H.-Y. Kee, *Phys. Rev. B* **81** (2010) 081105.
- [67] W.-C. Lee, D.P. Arovas, C. Wu, *Phys. Rev. B* **81** (2010) 184403.
- [68] U. Stockert, M. Abdel-Hafiez, D.V. Evtushinsky, V.B. Zabolotnyy, A.U.B. Wolter, S. Wurmehl, I. Morozov, R. Klingeler, S.V. Borisenko, B. Büchner, *Phys. Rev. B* **83** (2011) 224512.
- [69] G. Lehmann, M. Taut, *Phys. Status Solidi (b)* **54** (1972) 469–477.
- [70] S.A. Carter, B. Batlogg, R.J. Cava, J.J. Krajewski, W.F. Peck, L.W. Rupp, *Phys. Rev. B* **51** (1995) 17184–17187.
- [71] S. Nishizaki, Y. Maeno, S. Farner, S. ichi Ikeda, T. Fujita, *J. Phys. Soc. Jpn.* **67** (1998) 560–563.
- [72] S. Nishizaki, Y. Maeno, Z. Mao, *J. Low Temp. Phys.* **117** (1999) 1581–1585.
- [73] S. Nishizaki, Y. Maeno, Z. Mao, *J. Phys. Soc. Jpn.* **69** (2000) 572–578.
- [74] Y. Maeno, K. Yoshida, H. Hashimoto, S. Nishizaki, S. ichi Ikeda, M. Nohara, T. Fujita, A.P. Mackenzie, N.E. Hussey, J.G. Bednorz, F. Lichtenberg, *J. Phys. Soc. Jpn.* **66** (1997) 1405–1408.
- [75] Y. Maeno, H. Hashimoto, K. Yoshida, S. Nishizaki, T. Fujita, J.G. Bednorz, F. Lichtenberg, *Nature* **372** (1994) 532–534.
- [76] J.J. Neumeier, M.F. Hundley, M.G. Smith, J.D. Thompson, C. Allgeier, H. Xie, W. Yelon, J.S. Kim, *Phys. Rev. B* **50** (1994) 17910–17916.
- [77] A.P. Mackenzie, S. ichi Ikeda, Y. Maeno, T. Fujita, S.R. Julian, G.G. Lonzarich, *J. Phys. Soc. Jpn.* **67** (1998) 385–388.
- [78] N. Kikugawa, C. Bergemann, A.P. Mackenzie, Y. Maeno, *Phys. Rev. B* **70** (2004) 134520.
- [79] K. Pucher, J. Hemberger, F. Mayr, V. Fritsch, A. Loidl, E.-W. Scheidt, S. Klimm, R. Horny, S. Horn, S.G. Ebbinghaus, A. Reller, R.J. Cava, *Phys. Rev. B* **65** (2002) 104523.
- [80] J. Merino, R.H. McKenzie, *Phys. Rev. B* **62** (2000) 2416–2423.
- [81] C. Bergemann, J. Brooks, L. Balicas, A. Mackenzie, S. Julian, Z. Mao, Y. Maeno, *Physica B* **294–295** (2001) 371–374.
- [82] A.P. Mackenzie, S.R. Julian, A.J. Diver, G.J. McMullan, M.P. Ray, G.G. Lonzarich, Y. Maeno, S. Nishizaki, T. Fujita, *Phys. Rev. Lett.* **76** (1996) 3786–3789.
- [83] A. Mackenzie, S. Julian, A. Diver, G. Lonzarich, N. Hussey, Y. Maeno, S. Nishizaki, T. Fujita, *Physica C: Superconduct.* **263** (1996) 510–515.
- [84] S. Hill, J.S. Brooks, Z.Q. Mao, Y. Maeno, *Phys. Rev. Lett.* **84** (2000) 3374–3377.
- [85] T. Oguchi, *Phys. Rev. B* **51** (1995) 1385–1388.
- [86] D.S. Inosov, S.V. Borisenko, I. Eremin, A.A. Kordyuk, V.B. Zabolotnyy, J. Geck, A. Koitzsch, J. Fink, M. Knupfer, B. Büchner, H. Berger, R. Follath, *Phys. Rev. B* **75** (2007) 172505.
- [87] B.J. Taylor, M.B. Maple, *Phys. Rev. Lett.* **102** (2009) 137003.
- [88] S. Raghun, A. Kapitulnik, S.A. Kivelson, *Phys. Rev. Lett.* **105** (2010) 136401.
- [89] M. Sato, M. Kohmoto, *J. Phys. Soc. Jpn.* **69** (2000) 3505–3508.